Statyba

ISSN: 1392-1525 (Print) (Online) Journal homepage: https://www.tandfonline.com/loi/tcem19

CURVATURE ANALYSIS OF HIGH STRENGTH CONCRETE BEAMS

G. Kaklauskas PhD & M. Hallgren PhD

To cite this article: G. Kaklauskas PhD & M. Hallgren PhD (1999) CURVATURE ANALYSIS OF HIGH STRENGTH CONCRETE BEAMS, Statyba, 5:6, 357-363, DOI: 10.1080/13921525.1999.10531490

To link to this article: https://doi.org/10.1080/13921525.1999.10531490

Published online: 26 Jul 2012.

CURVATURE ANALYSIS OF HIGH STRENGTH CONCRETE BEAMS

G. Kaklauskas and M. Hallgren

1. Introduction

Concrete technology has developed rapidly during last decades. It is now quite common to use concrete with a compressive strength of 100 MPa or higher. High strength concrete seems to be an appropriate material to achieve higher, longer or more slender structures and to gain cost savings. However, current design codes for concrete structures are mainly based on tests where the concrete strengths have been below 60 MPa.

The shape of the stress-strain curve obtained from uniaxial compression tests of plain specimens is similar for concrete of normal, medium and high strength as shown in Fig 1. A high-strength concrete behaves in a linear fashion to a relatively higher stress level and has a higher strain at maximum stress than the low-strength concrete. On the descending portion of the stress-strain curve, higher strength concrete tends to behave in a more brittle manner, the stress dropping more sharply than it does for concrete with lower strength.

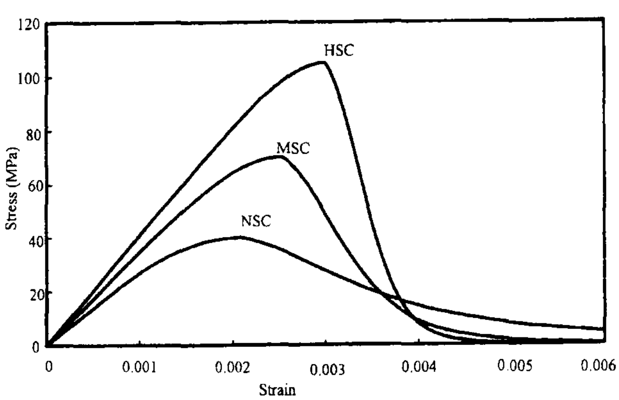

Fig 1. Typical stress-strain curves for normal (NSC), medium (MSC) and high strength concrete (HSC)

A number of complete stress-strain curves, both for normal and high strength concrete has been proposed. Mansur et al. [1] modified a complete stress-strain relationship of the serpentine curve proposed by Carreira and Chu [2]:

$$\sigma_c = \frac{f_c\, k_1\beta_c\left(\varepsilon_c / \varepsilon_0\right)}{k_1\beta_c - 1 + \left(\varepsilon_c / \varepsilon_0\right)^{k_2\beta_c}}, \qquad (1)$$

where

$$f_c = 0.94 f_c^{'},\ \ \varepsilon_0 = 0.0005(f_c)^{0.35},\ \ k_1 = (40/f_c)^2,$$

$$k_2 = (40/f_c)^{1.3},\ \ \beta_c = 1/\left(1 - f_c / \varepsilon_0 E_c\right),$$

$$E_c = 10300(f_c)^{0.33} \qquad (2)$$

Here σ_c and ε_c are respectively the stress and strain of compressive concrete; f_c and ε_0 are respectively the peak stress and strain for 100×100×200 mm prism; k_1 and k_2 are correction factors; β_c is a material parameter depending on the shape of the stress-strain diagram; and E_c is the initial tangent modulus.

Thorenfeldt et al [3] proposed a similar expression to Eq 1 for both normal and high strength concrete with the only difference of assuming $k_1 = 1$.

Recently a new constitutive relationship for cracked tensile concrete based on smeared crack approach has been proposed [4] for deformational analysis of flexural reinforced concrete members. The relationship has been developed on a basis of a number of stress-strain curves for tensile concrete [4-6] obtained from beam tests reported in literature. Accuracy of the proposed constitutive relationship has been investigated [7] by calculating deflections for a large number of experimental reinforced concrete beams with moderate and small reinforcement ratios reported by several investigators.

The paper is aimed at investigating deformational behaviour of high strength concrete beams subjected to short-term bending. The present work includes both experimentation and analysis. The experimental part has involved a set of load test data for flexural high strength concrete elements. In the analytical contribution, comparison of experimental curvatures with curvatures predicted by four methods is carried out.

2. Tests of reinforced concrete beams from high strength concrete

General

The second author at the Royal Institute of Technology, Sweden, conducted flexural tests of 26 reinforced concrete beams of normal and high strength concrete [8]. The compressive cube (150 mm) strength of concrete ranged from about 40 to 100 MPa. The beams were simply supported and subjected to short-term four-point bending. Present research deploys experimental data of 26 beams divided into three series: B90, B91 and B92. All the beams had a rectangular cross-section and were singly reinforced in the pure bending zone. Beams of series B90 were nominally 4.0 m long, 140 mm high and 150 mm wide (in the pure bending zone) while the corresponding characteristics for beams of series B91 and B92 were 5.2 m, 150 mm and 180mm. Measured cross-section dimensions and material strengths of the test beams are presented in Table 1.

Material properties

Concrete mix details are given in Table 2. The beams were cured covered with wet burlap sacks during the first five days and then in indoor climate in the laboratory with a relative humidity of about 70% and temperature of 20°C. Compressive strength of concrete (Table 1) was determined by tests on cylinders (300 mm height and 150 mm diameter) and cubes (150 mm). Number and diameter of deformed reinforcement bars as well as their yield stress are indicated in Table 1.

Testing arrangements

The test beams were supported on hinged roller supports which enabled free rotation and free horizontal displacement of the beams. The load was applied to the test beam with a servohydraulic actuator and transferred to the two loading points by a steel beam.

The longitudinal concrete strains in the mid section of the test beams were measured by five electrical resistance strain gauges glued to the beam surface. One of these gauges was placed centrally on the compressive surface and the other four at different levels on one side of the test beams with the extreme gauge distanced at 55 mm from the top. The strain in the tension reinforcement was measured in one bar in the mid section of the test beams. The bar was provided with two gauges glued to opposite sides. All gauges were of trade mark Showa and the lengths of the gauges for measuring concrete and steel strains were 30 and 8 mm, respectively.

The loading was controlled with a MTS 458.20 control console. The load was applied at a deformation rate of about 0.1 mm/s, measured on the movement of the piston rod, and in steps of 2.0 kN until the first crack was visually observed on the vertical side surfaces of the test beam. After the appearance of the first crack, the loading steps were increased to 4.0 kN. Between the loading steps, the piston rod was locked for about two minutes, during which the crack pattern was inspected and recorded. When the yield load of the beam was reached, the deformation rate was increased and the beam was loaded continuously until complete failure. The experimental results were presented in terms of moment-curvature $(M-\kappa)$, diagrams for 26 test beams [8].

3. Strain and curvature analysis technique

The present curvature analysis method is based on classical principles of strength of materials extended to layered approach and use of full material diagrams. It is based on the following assumptions of behaviour of flexural reinforced concrete members: 1) the hypothesis of plane sections of beam bending and the resulting linear distribution of strain within the depth of the beam section is adopted; 2) perfect bond between reinforcement and concrete is assumed; 3) the constitutive model is based on the smeared crack approach, ie stresses and strains are averaged over representative lengths to span several cracks.

According to the layered approach, the beam's cross-section is divided into a number of horizontal layers corresponding to either concrete or reinforcement. Each layer may have different material properties assumed to be constant over the layer thickness. Thickness of the reinforcement layer is taken from the condition of the equivalent area. For reinforcement material idealisation, a bilinear, trilinear or more complex stress-strain relationship can be adopted. The stress-strain relationship for the compressive concrete has been assumed according to Eqs (1) and (2) assuming $k_1 = 1$. The present analysis employs a stress-strain relationship for tensile concrete proposed by the first author [4]. The descending part of the relationship shown in Fig 2 has the expression:

$$\sigma_t = 0.625 f_t' \left(1 - \frac{\overline{\varepsilon_t}}{\beta} - \frac{1+0.6\beta}{\beta \overline{\varepsilon_t}} \right), \quad (3)$$

where

$$\overline{\varepsilon_t} = \frac{\varepsilon_t}{\varepsilon_t'}; \quad \varepsilon_t' = \frac{f_t'}{E_c}. \quad (4)$$

$$\beta = 32.8 - 27.6p + 7.12p^2, \quad (5)$$

$$\beta = 5, \text{ if } p \geq 2\%,$$

where p is reinforcement percentage. Tensile strength of concrete was taken as

$$f_t' = 0.23\sqrt[3]{R_{15}^2} \text{ [MPa]}, \quad (6)$$

where R_{15} is 150 mm cube compression strength.

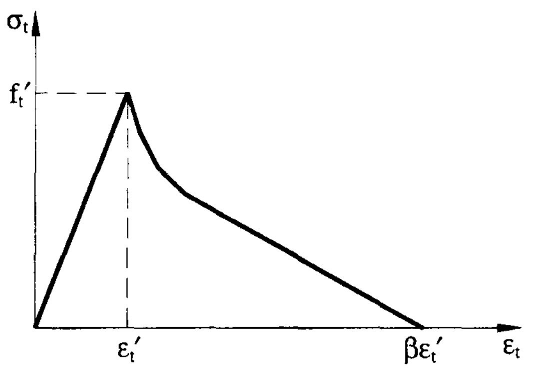

Fig 2. A stress-strain relationship for tensile concrete

A computer program has been developed for assessment of average stress and strain state at any point of the beam as well as for calculation of curvatures. For a given external moment, the computation is performed in iterations by the following steps:

1. In the first iteration, elastic material properties are assumed for all the layers.

2. Geometrical characteristics are calculated for the transformed cross-section.

3. Curvature of the section is calculated from the expression:

$$\kappa = \frac{M}{(EI)_{tr}}, \quad (7)$$

where $(EI)_{tr}$ is the flexural stiffness of the transformed cross-section.

4. Longitudinal strain at every layer i is taken as

$$\varepsilon_i = \kappa y_i, \quad (8)$$

where y_i is the distance of i layer from the centroid of the transformed cross-section.

5. For the assumed material diagrams (eg, Fig 2), stress σ_i corresponding to strain ε_i is obtained. A secant deformation modulus $\overline{E}_i = \sigma_i / \varepsilon_i$ is determined.

6. Values of the obtained secant deformation modulus $\overline{E_i}$ for every layer are compared with the previously assumed or computed ones. If the agreement is not within the assumed error limits, a new iteration is started from step 2.

7. After convergation of deformation modulus $\overline{E}_i$ for all the layers, final values of strains, stresses and curvature are computed.

4. Comparison of curvatures assessed by different methods with test results

This section compares predicted and experimental curvatures of 26 beams described in section 2 (Table 1). Curvatures were assessed not only by the method discussed above, but also by ACI [9] Eurocode [10], and Russian Code [9]methods.

Curvatures for all the beams were calculated at five moment levels, ie 0.4, 0.55, 0.6, 0.7 and 0.8 of M_u which is the experimental ultimate moment. The experimental (dashed lines) and computed by the present analysis method (solid lines) moment-curvature diagrams for the three series are presented in Fig 3. Although good agreement has been achieved for most of the beams, some tendency of underestimation of curvatures with increasing discrepancy at higher moments can be noted. The reason for that could be due to the following: 1) the computation has not assessed any plastic strains of reinforcement; 2) since most of the specimens were highly reinforced members, numerical curvature results corresponding to higher loads were very sensitive to variation of such factors as concrete strength and the shape of the descending branch of the stress-strain relationship for compressive concrete. Previous analysis [7] has shown that for moderately and lightly reinforced members neither concrete strength nor the shape of the descending branch of the compressive stress-strain relationship have significant influence on numerical results of deformations whereas the main factors are the modulus of elasticity of concrete as well as the stress-strain relationship for tensile concrete. For visualisation purposes, relative curvatures, $\kappa_{th} / \kappa_{\exp}$, versus relative moments are presented graphically in Fig. 4 where data points corresponding to different series are marked differently.

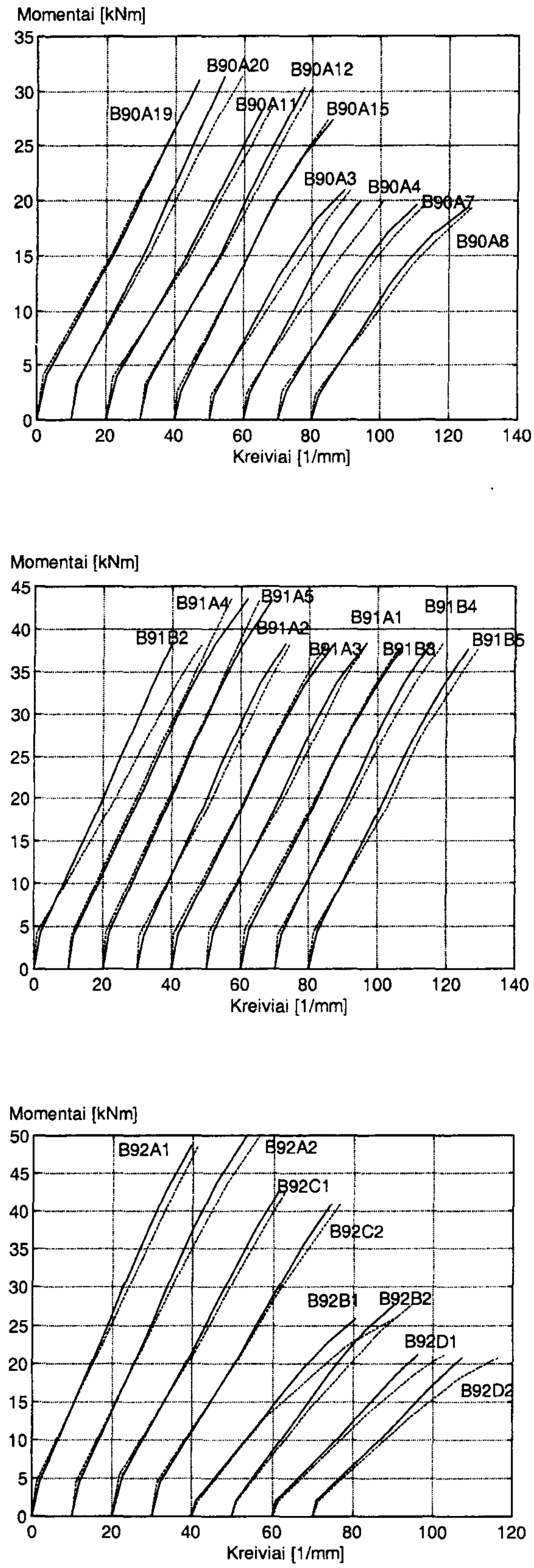

Fig 3. Moment-curvature diagrams ________ – computer, --------- – experimental

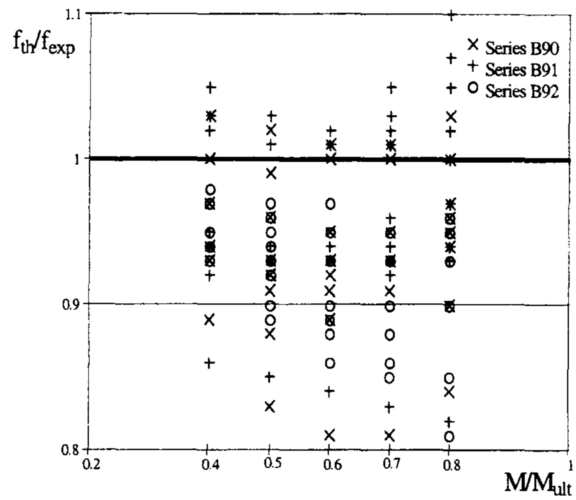

Fig 4. Present analysis predictions: relative deflections versus relative moments

Accuracy of predictions has been assessed using basic statistical parameters such as mean value and standard deviation calculated for relative curvatures. These statistical parameters assessed for predictions by the method of present analysis and ACI [9], Eurocode [10], and Russian Code [11] methods are presented Table 3. It contains the statistical parameters not only for the total data, but also for moment levels corresponding to 0.4, 0.6, and 0.8 of M_u.

An excellent agreement for the total data has been achieved for the present analysis, Eurocode and ACI methods with standard deviations for relative curvatures, $\kappa_{th} / \kappa_{exp}$, not exceeding 7.5% (Table 3). Even better results have been obtained for the moment level 0.4 M_u, but greater variation corresponded to 0.8 M_u. A tendency of the reduced mean value and its deviation from unity with increasing moments is clear for the ACI and Eurocode methods. Although predictions by the Russian Code method lead to a slightly greater standard deviation, the method gave a reasonable mean value.

Finally, it should be noted that better curvature predictions achieved in the present analysis by all the methods in comparison to the previous analysis [7] of reinforced concrete beams with low and moderate reinforcement ratios can be explained not only by high accuracy of the testing, but also by relatively insignificant role of tensile concrete due to high reinforcement ratio. When the influence of the tensile concrete (its strength) as a highly dispersed value is excluded, flexural deformability is mostly dependent on far more reliable characteristics such as modulus of elasticity of steel and concrete.

Table 1. Main characteristics of test beams

No	Beam	Depth [mm] h	Width [mm] b	Effective depth [mm] d	150 mm cube strength [MPa] R_{15}	Cylinder strength [MPa] f_c'	Tensile steel			Reinforcement ratio [%] P
							No and diameter of bars [mm]	Section area A_s $x10^{-4}[m^2]$	Yield strength f_{sy} [MPa]	
Series B90										
1	B90A3	145	151	112	41.0	32.8	3∅16	603	636	3.6
2	B90A4	145	155	113	41.0	32.8	3∅16	603	636	3.4
3	B90A7	139	159	108	38.6	31.1	3∅16	603	636	3.5
4	B90A8	140	157	105	38.6	31.1	3∅16	603	636	3.7
5	B90A11	139	153	105	97.0	86.2	3∅16	603	645	3.8
6	B90A12	140	155	106	97.0	86.2	3∅16	603	645	3.7
7	B90A15	142	164	113	51.5	44.9	3∅16	603	645	3.3
8	B90A19	140	157	107	100.5	84.6	3∅16	603	645	3.6
9	B90A20	141	156	110	100.5	84.6	3∅16	603	645	3.5
Series B91										
10	B91A1	151	180	108	72.4	65.7	2∅25	981	623	5.0
11	B91A2	150	180	110	73.4	61.8	2∅25	981	623	5.0
12	B91A3	150.5	180	107	73.4	61.8	2∅25	981	623	5.0
13	B91A4	151	182	108	80.4	69.1	2∅25	981	623	5.0
14	B91A5	152	180.5	110	80.4	69.1	2∅25	981	623	4.9
15	B91B2	152	183.5	115	83.0	60.8	4∅16	804	647	3.8
16	B91B3	150	182	111	72.4	65.7	4∅16	804	647	4.0
17	B91B4	150.5	181	114	69.7	58.3	4∅16	804	647	3.9
18	B91B5	150	183.5	112	69.7	58.3	4∅16	804	647	3.9
Series B92										
19	B92A1	154	176	112	90.4	76.7	3∅25	1473	623	7.5
20	B92A2	151	185	109	90.4	76.7	3∅25	1473	623	7.3
21	B92B1	153	180	113	47.5	42.1	3∅16	603	631	3.0
22	B92B2	156	180	117	47.5	42.1	3∅16	603	631	2.9
23	B92C1	156	178	113	90.4	76.7	2∅25	982	623	4.9
24	B92C2	151	179	108	90.4	76.7	2∅25	982	623	5.1
25	B92D1	155	185	118	47.5	42.1	2∅16	402	631	1.8
26	B92D2	151	181	116	47.5	42.1	2∅16	402	631	1.9

Table 2. Concrete mix proportions of test beams

Mix components	Unit	B90A11 B90A12	B90A15 B90A16	B90A19 B90A20	B91A1 B91B3	B91A2 B91A3	B91A4 B91A5 B91B4 B91B5	B91B1 B91B2	B92A1 B92A2 B92C1 B92C2	B92B1 B92B2 B92D1 B92D2
Portland cement, c	kg/m^3	499	510	411	450	450	400	450	429	430
Silica fume, s	kg/m^3	50	–	40	50	50	40	50	40	–
Crushed aggr. 8–18 mm	kg/m^3	905	860	990	1000	1000	940	1100	1070	805
Aggregate 0–8 mm	kg/m^3	930	910	970	900	900	960	800	1030	865
Water, w	kg/m^3	131	181	119	152	164	153	128	148	176
Superplasticizer	kg/m^3	33	–	18.1	20	20	15	26	18.3	–
Retarder	kg/m^3	5.5	–	6.8	5	5	4	5	5.1	–
w/(c+s)		0.24	0.36	0.26	0.30	0.33	0.35	0.26	0.31	0.41
Age at beam test, n	days	21	19	21	23	21	28	28	28	28

Table 3. Statistical parameters for relative curvatures, $\kappa_{th} / \kappa_{exp}$, estimated by different methods

No.	Characteristics of data	ACI		EC2		Russian Code		Present analysis	
		Mean	Stand.	Mean	Stand.	Mean	Stand.	Mean	Stand.
1.	0.4 M_u (26 points)	0.985	0.045	0.940	0.053	1.055	0.078	0.961	0.047
2.	0.6 M_u (26 points)	0.938	0.053	0.904	0.066	1.080	0.089	0.935	0.055
3.	0.8 M_u (26 points)	0.879	0.071	0.850	0.085	1.059	0.109	0.947	0.077
4.	Total (130 points)	0.935	0.066	0.900	0.075	1.069	0.092	0.944	0.059

5. Concluding remarks

A simple iterative technique based on classical principles of strength of materials extended to layered approach and use of full material diagrams have been applied to curvature analysis of 26 high strength concrete beams. Comparison with the experimental curvatures at five load levels and with estimates of three other methods has been performed. Accuracy of predictions has been assessed using basic statistical parameters such as mean value and standard deviation calculated for relative curvatures. An excellent agreement for the total data has been achieved for the present analysis, Eurocode and ACI methods with standard deviations not exceeding 7.5% (Table 3). Even better results have been obtained for the moment level 0.4 M_u, but greater variation corresponded to 0.8 M_u. A tendency of the reduced mean value and its deviation from unity with increasing moments is clear for the ACI and Eurocode methods. Although predictions by the Russian Code method lead to a slightly greater standard deviation, the method gave a reasonable mean value.

The present analysis method as a universal, simple and accurate tool for deformation analysis of flexural reinforced concrete members can serve as an alternative to the code methods.

References

1. M. A. Mansur, M. S. Chin and T. H. Wee. Flexural Behavior of High-Strength Concrete Beams // ACI Structural Journal, V. 94, No 6, November-December, 1997, p. 663–674.
2. D. J. Careira and K. -H. Chu. Stress-Strain Relationship of Reinforced Concrete in Tension // ACI Journal, 83(1), 1986, p. 21–28.
3. E. Thorenfeldt, A. Tomaszewicz and J. J. Jensen. Mechanical Properties of High-Strength Concrete and Application in Design. Procedings, Sympozium in Stavanger, Norway, 1987, p. 17–22.
4. G. Kaklauskas. A New Stress-Strain Relationship for Cracked Tensile Concrete in Flexure // Statyba, Vol V, No 6. Vilnius: Technika, 1999, p. 349–356.
5. G. Kaklauskas. A Technique for Investigation of Tension Stiffening Effect of Flexural RC Members // Proceedings, 10th Nordic Seminar on Computational Mechanics, Tallinn, Estonia, October 24–25, 1997, p. 228–231.
6. G. Kaklauskas, J. Ghaboussi and X. Wu. Neural Network Modelling of Tension Stiffening Effect for R/C Flexural Members // Proceedings, EURO-C 1998-Computational Modelling of Concrete Structures, Badgastein, Austria, March 31 – April 3, 1998, p. 823–832.
7. G. Kaklauskas, D. Bačinskas, R. Šimkus. Deflection Estimates of Reinforced Concrete Beams by Different Methods // Statyba, Vol V, No 4. Vilnius: Technika, 1999, p. 258–264.
8. M. Hallgren. Flexural and Shear Capacity of Reinforced High Strength Concrete Beams without Stirrups. Licentiate Thesis. Royal Institute of Technology, Stockholm, Sweden, 1994. 150 p.
9. ACI Committee 318. Building Code Requirements for Reinforced Concrete and Commentary (ACI 318-89/ACI 318R-89). Detroit: American Concrete Institute (ACI), 1989. 353 p.
10. ENV 1992-1-1.Eurocode 2: Design of Concrete Structures - Part 1: General rules and rules for buildings. Brussels, 1992. 114 p.
11. СНиП 2.03.01-84*. Бетонные и железобетонные конструкции. М.: Госстрой СССР. 1989. 80 с.

Įteikta 1999 10 27

STIPRAUS BETONO GELŽBETONINIŲ SIJŲ KREIVIŲ ANALIZĖ

G. Kaklauskas, M. Hallgren

S a n t r a u k a

Straipsnyje pateikti stipraus betono gelžbetoninių sijų deformatyvumo tyrimo rezultatai. Darbą sudaro dvi dalys: eksperimentinė ir teorinė.

Eksperimentinėje dalyje pateikti antrojo autoriaus Karališkajame technologijos institute (Švedijoje) atliktų bandymų [8] rezultatai. 26 laisvai atremtos gelžbetoninės sijos buvo išbandytos trumpalaike apkrova – dviem koncentruotomis jėgomis. Betono 150 mm kubelių stipris kito nuo 40 iki 100 MPa. Stačiakampio skerspjūvio sijos, grynojo lenkimo zonoje armuotos tik tempiama armatūra, buvo sudalytos į tris serijas: B90, B91, B92. B90 serijos sijos buvo 4,0 m ilgio, o skerspjūvio aukštis - 140 mm, plotis 150 mm. Atitinkami B91 ir B92 serijų sijų nominalūs matmenys buvo 5,2 m, 150 mm ir 180 mm. Sijų skerspjūvio ir betono mišinio charakteristikos pateiktos atitinkamai 1 ir 2 lentelėse.

Sijų gniuždomo betono deformacijos grynojo lenkimo zonoje buvo matuojamos penkiais 30 mm ilgio elektriniais tenzodavikliais, priklijuotais skirtinguose skerspjūvio aukščiuose. Armatūros strypų deformacijos buvo matuojamos 8 mm ilgio tenzodavikliais.

Teorinėje dalyje eksperimentinėms sijoms buvo apskaičiuoti kreiviai sluoksnių metodu ir palyginti su kitų žinomų analitinių metodų apskaičiavimo rezultatais. Skaičiuojant sluoksnių metodu, gelžbetoninio elemento skerspjūvis yra sudalijamas į horizontalius į betono ir armatūros sluoksnius. Skaičiuojama iteracijomis, taikant medžiagų atsparumo formules bei išsamias medžiagų diagramas. Gniuždomam betonui taikoma (1), o tempiamam betonui pirmojo autoriaus pasiūlyta (3) priklausomybė.

Kiekvienai sijai penkiuose apkrovos lygiuose (0,4, 0,5, 0,6, 0,7 ir 0,8 eksperimentinio ardančiojo momento M_u reikšmės) buvo apskaičiuoti kreiviai ir palyginti su eksperimentų rezultatais. Eksperimentinės (punktyrinė linija) ir teorinės (ištisa linija) momentų-kreivių diagramos visoms sijoms pateiktos 3 pav. Nors gautas neblogas teorinių ir eksperimentinių kreivių atitikimas, daugeliui sijų, esant didesnėms apkrovoms, apskaičiuoti kreiviai yra kiek mažesni už eksperimentinius. Tai matyti 4 pav., kuriame pateikta santykinių kreivių ($\kappa_{th} / \kappa_{\exp}$, kur κ_{th} yra teorinis, o $\kappa_{\exp}$ – eksperimentinis kreivis) priklausomybė nuo momento.

Be sluoksnių metodo, kreiviai dar buvo apskaičiuoti amerikietiškų [9], Euronormų [10] bei Lietuvoje galiojančių normų [11] metodais. Vertinant tikslumą, kiekvienu skaičiavimo metodu nustatytiems santykiniams kreiviams buvo gauti tokie svarbiausi statistiniai dydžiai kaip vidurkis bei vidutinis kvadratinis nuokrypis. Statistinio apskaičiavimo rezultatai pateikti 3 lentelėje. Sluoksnių, Euronormų ir amerikietiškų normų metodais apskaičiuotiems kreiviams vidutinis kvadratinis nuokrypis, nustatytas visiems eksperimento taškams (visos sijos, 5 apkrovos lygiai), neviršija 7,5%. Apkrovos lygiui 0,4 M_u vidutinis kvadratinis nuokrypis dar mažesnis, tačiau jis yra didesnis apkrovos lygiui 0,8 M_u. Reikia pažymėti, kad Euronormų ir amerikietiškų normų metodams gauta kiek didesnė sisteminė paklaida nei sluoksnių metodui, ypač didesniems apkrovos lygiams. Lietuvoje galiojančių normų metodui gauta sisteminė paklaida yra apytikriai tokia kaip kitų metodų, tačiau vidutinis kvadratinis nuokrypis kiek didesnis. Apskritai imant, toks geras apskaičiuotų ir eksperimentinių kreivių sutapimas visiems metodams gali būti paaiškintas ne tik eksperimento kokybe, bet ir maža tempiamo betono įtaka šių stipriai armuotų sijų deformatyvumui.

Gintaris KAKLAUSKAS. PhD, Senior Researcher and Associate Professor. Dept of Reinforced Concrete Structures, Vilnius Gediminas Technical University, Saulėtekio al. 11, 2040 Vilnius, Lithuania.

Graduate of Vilnius Civil Engineering Institute (presently Vilnius Gediminas Technical University, VGTU), 1982 (civil engineer). PhD (1990). Research visits: Aalborg University (Denmark, 1991), University of Glamorgan (UK, 1994/1995, 1998), University of Illinois, Urbana-Champaign (USA, 1996). Author and co-author of 2 monographs, 1 invention and a number of papers. Research interests: development of constitutive relationships for concrete and numerical simulation of reinforced concrete structures.

Mikael HALLGREN. PhD, Structural Engineer, Head of Civil Engineering Department, Scandiaconsult, AB, PO Box 4205, SE-102 65 Stockholm, Sweden.

Graduate of the Royal Institute of Technology, MSc (civil engineering, 1989), (Licentiate of Eng. 1994), Doctor of Techn., PhD (1996). Author of 2 monographs, and author and co-author a number of papers and reports. Research interests: high strength concrete structures, flexural capacity, shear and punching shear, shock-wave loading, and numerical simulation of reinforced concrete structures.